Advances in Computational Design, *Vol. 7, No. 3 (2022) 189-210*
https://doi.org/10.12989/acd.2022.7.3.189

A class of actuated deployable and reconfigurable multilink structures

Marios C. Phocas*[1], Niki Georgiou[1a] and Eftychios G. Christoforou[2b]

[1]*Department of Architecture, Faculty of Engineering, University of Cyprus, 75 Kallipoleos Str., P.O. Box 20537, 1678 Nicosia, Cyprus*
[2]*Department of Mechanical and Manufacturing Engineering, Faculty of Engineering, University of Cyprus, 75 Kallipoleos Str., P.O. Box 20537, 1678 Nicosia, Cyprus*

(Received December 28, 2020, Revised July 14, 2021, Accepted January 26, 2022)

Abstract. Deployable structures have the ability to shift from a compact state to an expanded functional configuration. By extension, reconfigurability is another function that relies on embedded computation and actuators. Linkage-based mechanisms constitute promising systems in the development of deployable and reconfigurable structures with high flexibility and controllability. The present paper investigates the deployment and reconfigurability of modular linkage structures with a pin and a sliding support, the latter connected to a linear motion actuator. An appropriate control sequence consists of stepwise reconfigurations that involve the selective releasing of one intermediate joint in each closed-loop linkage, effectively reducing it to a 1-DOF "effective crank–slider" mechanism. This approach enables low self-weight and reduced energy consumption. A kinematics and finite-element analysis of different linkage systems, in all intermediate reconfiguration steps of a sequence, have been conducted for different lengths and geometrical characteristics of the members, as well as different actuation methods, i.e., direct and cable-driven actuation. The study provides insight into the impact of various structural typological and geometrical factors on the systems' behavior.

Keywords: deployable structures; effective crank-slider method; finite-element analysis; linkage structures; motion planning; reconfigurable structures

1. Introduction

Deployable structures are capable of transforming from a packaged or compact state into an expanded functional configuration to serve temporary purposes, while connotating a small storage volume and easy transportability (Jensen 2005, Doroftei *et al.* 2014). By extension, deployable structures, that are also reconfigurable, are capable of further adjusting their shape through motion control and changing functional, environmental, or loading conditions. Relevant reconfigurations may help to meet certain objectives related to improved space utilization, indoor acoustics,

*Corresponding author, Professor, E-mail: mcphocas@ucy.ac.cy
[a]Ph.D. Student, E-mail: georgiou.niki@ucy.ac.cy
[b]Assistant Professor, E-mail: e.christoforou@ucy.ac.cy

http://www.techno-press.org/?journal=acd&subpage=7 ISSN: 2383-8477 (Print), 2466-0523 (Online)

lighting conditions, sun protection, natural ventilation, renewable energy efficiency, as well as reduced external loading (Christoforou *et al.* 2015). Meanwhile, advances in digital and numerical computing technologies open up new research opportunities for related effective and practical morphological, structural and control engineering investigations.

The development of deployable and reconfigurable building structures is enhanced by applying specific design aspects and enabling increased performance with minimum means. Such aspects relate to minimum self-weight which serves to minimize the members' internal stresses, modularity enhancing the system's connectivity, expandability and constructability, and shape for controlled configurability conditions (Phocas *et al.* 2015). Tensegrity, scissor-like and origami systems have been developed in the past years for various architectural and engineering applications, at first place involving deployability (Pellegrino 2001, Hanaor and Levy 2001, Li *et al.* 2019).

Tensegrity structures comprise interconnected spatial self-stressed units of compression members that are only connected through tension members (Snelson 1965, Pugh 1976, Bel Hadj *et al.* 2011), or directly joined consecutively and stabilized through tension members, e.g., bar-to-bar connections (Djouadi *et al.* 1998). Tensegrity structures have proven to have adequate stiffness under external loads, and may be actively controlled based on their own members' properties (Gantes 2001). The direct implementation of linear motion actuators in place of compression members, or tension members of variable length, enables the system to obtain shape transformation attributes (Hanaor 1998, Tilbert 2002, Adam and Smith 2008). Relevant deployability studies have been presented in (Motro *et al.* 2001).

Scissor-like elements consist of a pair of bars interconnected with a rotational joint (Escrig 1985, You and Pellegrino 1997, Maden *et al.* 2011). During deployment, the system acts as a structural mechanism. The geometrical characteristics of the system, i.e., the joint location and bars' length, determine the transformation course and the target configuration at the deployed state. The stabilization of the system requires 'locking' techniques or additional members to be connected in parallel at the upper and lower end-nodes of the bars (Gantes 2001, Richard Liew *et al.* 2008). Similar kinetic system typologies include symmetrical assemblies of over-constrained bar mechanisms (Gan and Pellegrino 2003, Chen and You 2008,).

Origami structures of rigid plates consist of hinge-like creases with highly concentrated deformation and link-like facets with practically no deformation during folding. Thus, the rigid origami pattern forms a combination of corresponding linkages, and the admissible degree-of-freedom (DOF) is limited to rigid folding. A comprehensive kinematic model for rigid origami is developed in (Chen *et al.* 2015) by identifying a kinematically equivalent spatial linkage model. By extension, systematic and easy-to-implement approaches that can effectively generate new origami patterns, such as the computational method, gain significance for automatically assigning mountain-valley fold lines to given geometric configurations of origami structures (Chen *et al.* 2020), and the geometric-graph-theoretic representation of origami of regularly repeated folding patterns (Chen *et al.* 2021). Furthermore, hybrid typologies have been developed with a view to improve the kinematics and constructability of origami structures of rigid plates, such as the so-called origami-scissor hinged system, whereas the origami rigid plates are replaced by scissor-like elements (Rivas-Adrover 2018), as well as the deployable origami arch of rigid plates that is multi-stable and inflatable (Melancon *et al.* 2021).

While deployable structures often provide only individual target system configurations, reconfigurability is principally enabled through replacement of primary members with actuators, which often leads to increased structural weight, complex mechanisms and energy-inefficient

operation. In an effort to reduce the number of embedded actuators used in tensegrity structures, the so-called strut-routed actuation of interconnected compression members has been proposed (Moored and Bart-Smith 2009, Moored *et al.* 2011, Rhode-Barbarigos 2012). The actuators may even be placed outside the structure, provided that they are linked with continuous cables and spring elements, running through a series of connected struts and pulleys at the nodes (Schenk *et al.* 2007). However, the system requires a higher number of controlled members, and connection spacing becomes critical, since numerous active cables need to be routed through the same strut paths. In scissor-like elements, configurational variability is possible through simple angulated elements (Hobberman 1993, You and Pellegrino, 1997), scissor-hinge mechanisms (Akgün *et al.* 2010, Akgün *et al.* 2011), and universal scissor components (Allegria Mira *et al.* 2015). Further developments involve the implementation of scissor-like elements in deployable and transformable grid structures, such as translational scissor units based on any planar circle packing (Roovers and De Temmerman 2017), forming reciprocal linkages (Pérez-Valcárcel *et al.* 2021), and three-dimensional angulated scissor units based on a regular polygonal base (Krishnan and Liao 2020). In this context, a cylindrical net-shell deployment mechanism of a truss, which can fit different possible cylindrical surface shapes in the deployed state, was proposed for application purposes in the space industry (Lin *et al.* 2019). Further variability is possible through coupling of scissor-like elements with bending-active members (Phocas *et al.* 2019). In this case, the kinematics of the system is primarily based on the mechanical properties of the members that enable actuation and structural shape alteration through their own deformability.

By extension, linkage-based systems, which comprise continuous series of one-dimensional, rigid bars interconnected by lower-order pairs (Thrall *et al.* 2012), constitute promising systems in the development of deployable and reconfigurable modular structures with high flexibility and controllability. The linkage bars consist of single members, or may be further developed into hybrid elements so that the secondary members obtain a dual function, namely, participate in the load-transfer and actuation. In terms of the load-transfer mechanism, hybridization of the structure through a secondary system of struts and cable segments, i.e., cable-stiffened structure yields self-weight reduction while maintaining buckling length of the primary members (Schlaich *et al.* 2005, Engel 2009). The structural properties of the primary members are affected by the relative stiffness of the secondary system, in particular, the amount of prestress assigned to the tension members (Saitoh and Okada 1999). The use of continuous cables instead of segments, reduces the positive influence on the primary members, due to the constant axial force in the cables. Nevertheless, in terms of the system control, continuous cables of variable length are directly tensioned by a reduced number of motion actuators so that the structure may undergo respective shape changes.

For any system of interconnected links, the mobility analysis calculates the number of available DOF, which defines its nature (Norton 2008): (1) A positive number of DOF denotes a mechanism, i.e., relative motion is allowed between the members, (2) Exactly zero DOF represents the case of a structure, whereby no motion is possible, (3) A negative number of DOF corresponds to a preloaded structure, whereby no motion is allowed and possibly some stresses during assembly. Mobility is a determining factor for a mechanism and various formulas have been proposed in relevant literature for its calculation (Gogu 2005). In fact, these formulas have to be used with caution since they may not apply to specific mechanisms. In some cases, mobility analysis can be rather complex (Chen *et al.* 2017). The notion of mobility is central to the structural and reconfiguration concept applied to a family of reconfigurable building structures relevant to the present work.

In providing multiple possible target configurations, the reconfigurability of modular linkage

structures, with either direct or cable-driven actuation, has been investigated in simulations and experimentally (Phocas *et al.* 2012, 2015, 2019, Matheou *et al.* 2018, Christoforou *et al.* 2019). In the above studies, reconfigurations of pin-supported systems are based on the "effective 4–bar" (E4B) mechanism concept, i.e., a sequence of 1-DOF motion steps through selectively releasing two intermediate joints of the primary members, in order to stepwise adjust the system joints to the desired values. Similarly, deployability and reconfigurability of modular linkage structures, with a pin and a sliding support connected to a linear motion actuator, are based on the "effective crank–slider" (ECS) mechanism (Phocas *et al.* 2020). Again, an appropriate control sequence is used for stepwise reconfigurations. Each intermediate step involves the selective release of one intermediate joint in each closed-loop linkage effectively reducing it to a 1-DOF crank-slider mechanism. Both proposed kinematics approaches rely on a reduced number of actuators, positioned at the supports and detached from the main structure body, aiming to maintain minimum self-weight, structural simplicity and reduced energy consumption.

In extending the design potential of deployable and reconfigurable linkage structures, three system typologies of a 6 and 9-bar system, were examined in their deployment from an initial, almost flat configuration to a specific target one (Georgiou and Phocas 2020). These include a bar linkage (simple system - SS), a bar linkage with a secondary system of struts and parallel continuous cables to the links (hybrid system - HS) and diagonal continuous ones (cross hybrid system - CHS). Along these lines, this paper pursues a systematic investigation of three groups of aluminum bar linkages in the three typologies. The systems have a length of 9.0, 12.0 and 15.0 m in their initial, almost flat configuration, and a respective span of 4.5, 6.0 and 7.5 m in their specific arch-like target configuration. In each system the length of the bars amounts to 1.5, 1.0 and 0.75 m, respectively. In the hybrid structures, the struts have a reduced overall length of 1 m, compared to 1.5 m applied in the previous study. The investigation refers to the kinematics and the finite-element analysis (FEA) of the systems in all reconfiguration steps of a respective sequence. The results obtained refer to the actuator's forces, sliding distances of the rolling support and relative cable length variations, as well as to the criteria of highest maximum bending moments and inner forces in the members and vertical system deformations. The maximum bending moments of the members are indicative of the required brake torques on the joints of the linkages. Thus, the study provides insight into the impact of various factors on the systems behavior, such as structural typology, number and geometrical characteristics of the primary members.

2. Effective crank-slider approach

A planar linkage system constitutes the basic structural and kinematics element, consisting of n-serially connected rigid links with pivot joints in-between, as shown in Fig. 1. The structure is supported on the ground, through a pivot joint on one end and a linear sliding block on the other. Each intermediate joint is equipped with brakes. In a simple bar linkage, a linear actuator is fixed to the sliding block on the ground. In a hybrid system, a linear actuator is connected to each one of the continuous cables of variable length, while brakes are installed on the sliding block which are activated once an intermediate configuration step has been completed. The reconfiguration of the structure is based on stepwise adjustments of the joints, where in each step, the brake of one intermediate joint is selectively released, while the pin supports at the base are always kept unlocked. Following an appropriate scheduling sequence, every angle of the n-bar linkage system is adjusted to its target position step by step, converting the mechanism into a generic 1-DOF system, i.e., an ECS system. A reconfiguration of the mechanism can be achieved through

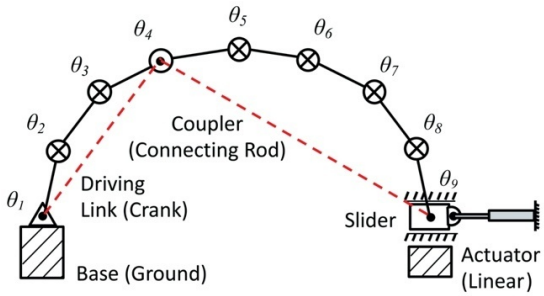

Fig. 1 ECS approach that is the basis for the stepwise deployment and reconfigurations of the system with a number of serially connected rigid links – 8 in the specific example (⊗: locked joint, Θ: unlocked joint, △: pivoted-to-the-ground joint, □: slider joint, —: physical link, – –: effective link) (Phocas *et al.* 2020)

different control sequences and an optimal one can be selected based on specific criteria, such as maximum required brake torques, actuator motion, etc. In the case of a system with n bodies (including the ground and the slider block), a complete reconfiguration will require a number of (n−3) intermediate steps, given that -during the final step- the four remaining variables (i.e., three joints and the slider position) will be adjusted simultaneously.

Despite the relative simplicity of the considered structural mechanism, it is important to proceed with a mobility analysis. The aforementioned approach is based on the fact that the proposed linkage structure is a closed-loop mechanism, for which the joint variables are subject to geometric loop-closure constraints that relate the joint variables. For this reason, the number of DOF of the system is less than the number of joints. In general, the number of DOF for a planar system is given by Gruebler's condition (Norton, 2008): $M = 3(L-1) - 2J_1 - J_2$, with L: number of links, J_1: number of 1-DOF joints, and J_2: number of 2-DOF joints. The above mechanism consists of n joints, (n-2) interconnected links and a slider: L=n (including the ground and the sliding block), J_1=n, J_2=0, and the number of DOF becomes M=n-3. When application of the brakes forms the mechanism, an ECS (n=4), the number of DOF becomes M=1. In principle, one motion actuator suffices for motion control purposes.

The proposed kinematics mechanism is expected to require reduced energy consumption for a reconfiguration of the system compared to a corresponding linkage with multiple motion actuators installed on the joints, given that the number of actuators must be equal to the number of DOF. In such a case, the actuators constitute additional lumped masses on the joints, thus increasing the self-weight of the structure and the energy consumption during reconfigurations.

Motion planning, i.e., definition of the scheduling sequences, plays a significant role in the verification of the geometry and dimensions of the linkage (Acharyya and Mandal 2009, Phukaokaew *et al.* 2019) and the avoidance of kinematic bifurcations (Chen *et al.* 2018, Park and Kim 1999). As part of motion planning, it is important to ensure that all intermediate configurations, including the transitions between them, avoid passing through singular configurations or their vicinity. This would be the case when, for example, the ECS mechanism acquires a fully extended or retracted position and the slider may not move any further. Accordingly, a perfectly aligned, flat bar linkage structure cannot be transformed by the horizontal actuator's force. Although the proposed implementation of the ECS method in the bar linkage structure involves only a primary linear motion actuator associated with the slider block, an auxiliary actuator installed at the base rotational joint could be added in, effectively preventing the mechanism from entering into an unwanted bifurcation path. The auxiliary actuator may also be

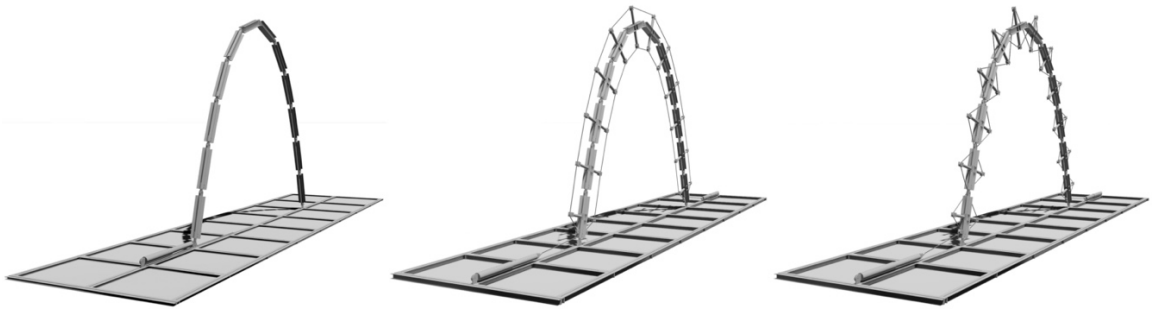

Fig. 2 Perspective view of 12-bar linkage, SS, HS and CHS, with 12 m overall length

used for load-sharing purposes. Although this is a topic raised in the present paper, it falls outside the central scope of the present research.

In the hybrid bar linkage structures, a motion actuator is associated with each of the continuous cables and the slider block is equipped with brakes. The hybrid structures cannot be fully extended, i.e., laid down flat, which can be practically limiting on site. A key feature of this actuation approach is that the control action, i.e., the reconfiguration force applied by the actuator, is also distributed to intermediate joints of the ECS, rather than being concentrated on the slider. In order to ensure smooth transition between the intermediate reconfiguration steps, a cable pretension needs to be appropriately applied, so that the active cable is readily engaged upon the brakes release. Pretensioning on the other cable is also necessary to prevent cable slack. In principle, when both cables are actuated at the same time, it makes the ECS system redundantly actuated (Müller 2013). As a consequence, the redundant actuation, through the two cables, enables the development of antagonistic forces that may generate internal pretension within the system, which would have to be balanced by the brakes, and be strategically controlled, in order to adjust the system stiffness (Müller 2005, Fontes and da Silva 2016).

3. Simulation study

A spatial skeleton structure consists of identical planar linkages placed in parallel in the longitudinal direction. The planar linkages are rigidly interconnected through secondary members to ensure adequate stiffness in the longitudinal planes of the spatial system. Thus, the overall shape of the structure is to be obtained from identical and synchronous reconfigurations of the individual planar linkages. The present paper focuses on the basic planar systems, as shown in Fig. 2.

The simulation study refers to the preliminary kinematics and the finite-element analysis of three groups of planar linkage systems. Each system group with identical initial length and target span is differentiated according to the number of bars and the linkage typology applied, i.e., SS, HS and CHS. Once the specific sequence for the stepwise reconfiguration of the systems has been applied, structural analysis involves the systems behavior under self-weight. FEA comprises a sequence of runs at snapshots corresponding to all individual completed configuration steps of the systems with all joints locked, from the initial to the target position. The transition between the individual configurations has not been considered, as it is assumed that only slow motions are involved, i.e., inertial effects are negligible. The simulation study and FEA are based on actual-size models to provide a realistic indication regarding the required control effort.

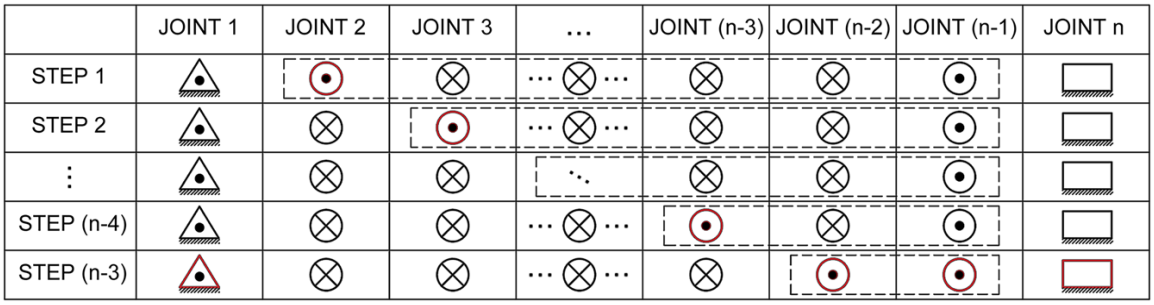

Fig. 3 Scheduling table for the control sequence principle of a linkage with n joints and (n-2) serially connected members, based on the ECS approach (⊗: locked joint, Θ: unlocked joint, △: pivoted–to–the-ground joint, □: slider joint). Dashed-line encirclements denote the effective coupler links. The red-colored symbols represent the currently adjusted joints

3.1 Motion planning

The primary members of the linkages consist of rigid aluminum bars of 1.5, 1.0 and 0.75 m length and a sliding block. The systems have an overall length of 9.0, 12.0 and 15.0 m in their initial, almost flat configuration, a respective span of half their initial length in their symmetric arch-like target configuration and three different respective numbers of bars depending on their individual length. The height of the systems in the target positions differs according to the number of bars used in each case. The general scheduling table for the stepwise reconfigurations of the bar linkages of each group of investigation with n joints and (n-2) bars, based on the ECS mechanism is depicted in Fig.3. The specific sequence order scheduled follows a clockwise joints adjustment, while the left ground support remains unlocked throughout the reconfiguration process (e.g., a case where the structure is not installed with brakes at the particular joint) and the right ground support is connected to the slider block.

3.2 Kinematics analysis

All planar linkages investigated consist of serially interconnected members with rotational joints in-between, which have the ability to lock and unlock at each transformation step, as required for the implementation of the scheduling sequence. Each linkage group with (n-2) number of bars has a reconfiguration that involves an initial form, $\theta_{ix,n-2}$, and a target configuration, $\theta_{fx,n-2}$. Table 1 includes the configurations defined by the position vectors, which include the internal joint angles of each linkage. Each linkage group corresponds to different values of L_i (length of the linkage when fully extended), L_f (span of the system, i.e., distance between the ground supports) and the number of bars.

The deployment process of the systems is achieved by selectively releasing one intermediate joint at each step. In the SS, one linear motion actuator is associated with the sliding block connected to the right support. Once the specific joint is adjusted, through a respective displacement of the sliding block by the linear motion actuator, it remains locked. The process is repeated until all joints of the system are adjusted. Once a target position has been obtained, the actuator locks in place.

In the hybrid systems, HS and CHS, cables are directly connected to linear motion actuators

Table 1 Bar linkages initial and target configurations

Linkage group 1: L_{i1}= 9.0 m, L_{f1}= 4.5 m, Number of bars: 6, 9, 12
$\Theta_{i1,6}$= [5, 175, 180, 180, 180, 180, 0]^T
$\Theta_{f1,6}$= [74, 171, 151, 108, 151, 171, 74]^T
$\Theta_{i1,9}$= [5, 175, 180, 180, 180, 180, 180, 180, 180, 0]^T
$\Theta_{f1,9}$= [76, 175, 172, 161, 136, 136, 161, 172, 175, 76]^T
$\Theta_{i1,12}$= [5, 175, 180, 180, 180, 180, 180, 180, 180, 180, 180, 180, 0]^T
$\Theta_{f1,12}$= [76, 177, 176, 173, 166, 152, 140, 152, 166, 173, 176, 177, 76]^T
Linkage group 2: L_{i2}= 12.0 m, L_{f1}= 6.0 m, Number of bars: 8, 12, 16
$\Theta_{i2,8}$= [5, 175, 180, 180, 180, 180, 180, 180, 0]^T
$\Theta_{f2,8}$= [75, 175, 169, 150, 122, 150, 169, 175, 75]^T
$\Theta_{i2,12}$= [5, 175, 180, 180, 180, 180, 180, 180, 180, 180, 180, 180, 0]^T
$\Theta_{f2,12}$= [76, 177, 176, 173, 166, 152, 140, 152, 166, 173, 176, 177, 76]^T
$\Theta_{i2,16}$= [5, 175, 180, 180, 180, 180, 180, 180, 180, 180, 180, 180, 180, 180, 180, 180, 0]^T
$\Theta_{f2,16}$= [76, 178, 177, 176, 175, 171, 166, 156, 150, 156, 166, 171, 175, 176, 177, 178, 76]^T
Linkage group 3: L_{i2}= 15.0 m, L_{f1}= 7.5 m, Number of bars: 10, 15, 20
$\Theta_{i3,10}$= [5, 175, 180, 180, 180, 180, 180, 180, 180, 180, 0]^T
$\Theta_{f3,10}$= [76, 176, 174, 167, 151, 132, 151, 167, 174, 176, 76]^T
$\Theta_{i3,15}$= [5, 175, 180, 180, 180, 180, 180, 180, 180, 180, 180, 180, 180, 180, 180, 180, 0]^T
$\Theta_{f3,15}$= [76, 178, 177, 176, 173, 169, 161, 150, 150, 161, 169, 173, 176, 177, 178, 76]^T
$\Theta_{i3,20}$= [5, 175, 180, 180, 180, 180, 180, 180, 180, 180, 180, 180, 180, 180, 180, 180, 180, 180, 180, 180, 180, 0]^T
$\Theta_{f3,20}$= [76, 178, 178, 178, 177, 176, 174, 171, 166, 159, 154, 159, 166, 171, 174, 176, 177, 178, 178, 178, 76]^T

and brakes are also installed on the sliding block. Only one of the two cables in these systems needs to be tensioned for the transfer of motion to the actuated joint to enable adjustments at each step, namely, in the HS, the lower one, and in the CHS, the one that passes through the lower strut next to the fixed support. The other cable only needs some pretention to remain stretched. However, application of two individual cables, and their corresponding actuators, enables the system to reconfigure to further target positions and also adjust its stiffness.

In the examples under investigation, the following requirements are considered:

• In the SS, every rotational joint is installed with brakes except for the two joints at the base.

• In the HS and CHS, every rotational joint is installed with brakes except for the one of the pin support.

• In the SS, the only actuated joint is the last joint, which is linear and associated with the sliding block.

• Joint position adjustments start from the left side of the linkage and move towards the right.

• During each reconfiguration step, one joint angle is completely adjusted to its target value.

• No rigid bar can move below the horizontal ground level.

• In the HS, the cables should remain above and below the rigid bars, respectively.

• In the CHS, an upper limit of 175^0 of any unlocked joint angle is imposed to avoid infeasible sequences.

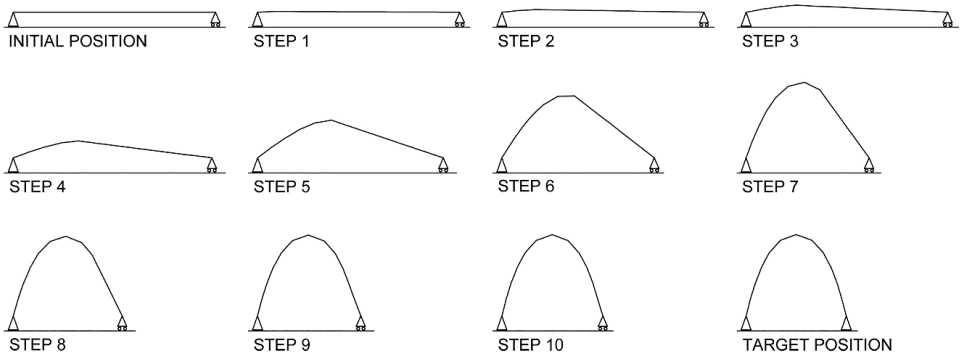

Fig. 4 Deployment sequence of the 12-bar-linkage, SS, with 12 m overall length

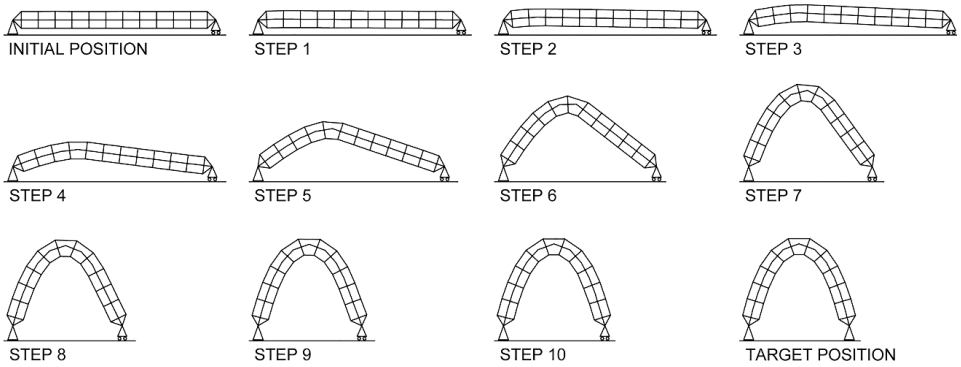

Fig. 5 Deployment sequence of the 12-bar-linkage, HS, with 12 m overall length

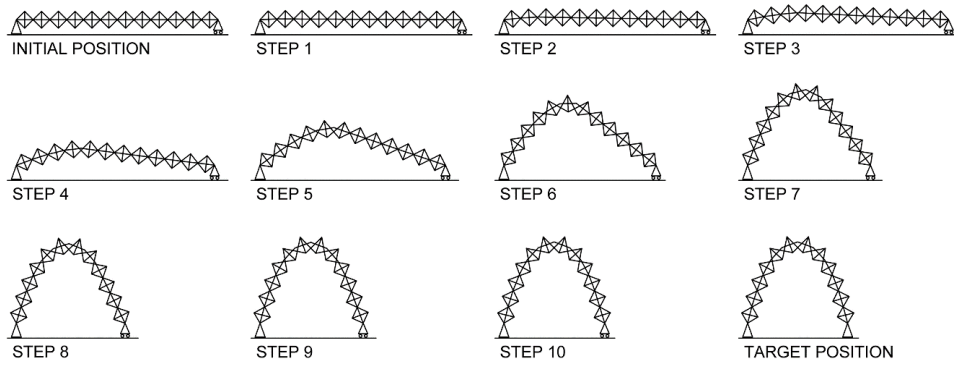

Fig. 6 Deployment sequence of the 12-bar-linkage, CHS, with 12 m overall length

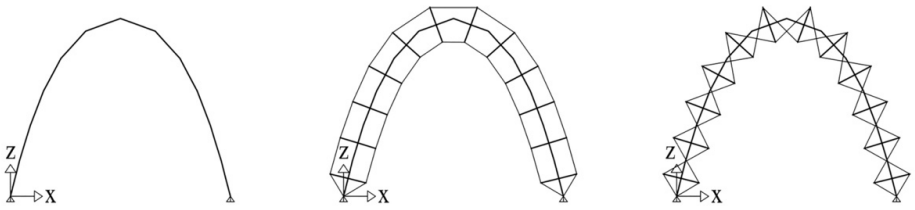

Fig. 7 FEA model of 12-bar-linkage, SS, HS and CHS, with 12 m overall length

The kinematics analysis of the planar bar linkages has been conducted with the software program Working Model 2D. The kinematics analysis was based on numerical integration of the linkage model, based on the Kutta-Merson method. The respective time step is automatically adjusted during the course of the simulation. The deployment steps of the planar 12-bar linkage of 12.0 m initial length in all three typologies are shown in Figs. 4-6.

3.3 Structural analysis

The beams of the planar linkages consist of pairs of UPN140/60 aluminum sections joined together. In the hybrid typologies, the struts consist of circular hollow sections of 60.3/4.6 mm and the cables, of 2 cm diameter. The struts are symmetrically positioned and rigidly connected to the beams. In the HS, the cables pass between pairs of pulleys positioned vertically at both ends of the struts, in the CHS, through single pulleys. The cables travel along the structure with one end anchored to the fixed support and the other end connected to a corresponding linear actuator. The self-weight of the beams amounts to 5.5 kg/m, the struts, 1.13 kg/m, and the cables, 2.5 kg/m.

FEA of the systems in each completed reconfiguration step was conducted using the software program SAP2000. The FEA models corresponding to the system configurations in the target position are shown in Fig. 7. In all system configurations, the supports are assumed to act as pin connections. The systems are considered to be of aluminum members of 69.6 GPa elastic modulus and 241.3 MPa yield strength. The cables in the hybrid systems are assigned to steel S450 of 24.82 GPa elastic modulus, and a pretension of 2 kN. The specific value of the cables pretension was found appropriate for the actuation requirements (as discussed in Section 2), while obtaining reduced system deformations in the target position under external loading. Each system is modeled as a set of idealized elements interconnected at the nodes, and the cables, as cable elements with undeformed length to account for their continuous course between the supports. Furthermore, no geometric imperfections, nor any initial deformation of the systems in each configuration step, have been considered. The conducted static structural analysis considers only the geometrical nonlinearity of the systems and their self-weight. In all cases, the response of the systems was within the elastic range.

The linkages have been categorized as to their overall length of 9.0, 12.0 and 15.0 m in their initial, almost flat configuration. The target span of the systems amounts to 50 % of their respective initial length. The system categorization includes three subgroups based on the bar length, i.e., 1.5, 1.0 and 0.75 m. All systems have been analyzed in three different typologies, i.e., SS, HS and CHS. The systems are characterized by the structure volume, V_S, and the enclosed area between the lower members (i.e., the beams of SS and the lower cables of HS and CHS) and the ground, A_S, at the deployed state, as well as their self-weight, W. The analysis results refer to the maximum actuator's force, F_a, sliding block displacement, Δl, and relative cable length variation, Δl_c. Results additionally include data concerning the highest maximum bending moment, M, shear force, Q, and axial force, N, of the members and vertical deformation of the system, U. All corresponding analysis results are recorded after completion of each reconfiguration step, i.e., with all internal joints locked. The comparative analysis refers to the systems of same typology within each group of given initial length and different number of bars, and the systems of each group of same initial length. Furthermore, the analysis results refer to the dependency of the system typologies of same individual bars length to the respective increase of the number of units.

Table 2 presents the main characteristics of the systems with regard to the volume of the structure, the enclosed area between the lower members and the ground at the deployed state, the self-weight, as well as the respective maximum actuator's force required for the reconfiguration,

Table 2 Analysis results of bar linkages: Initial system length, L_i, deployed structure volume, V_S, and enclosed area A_S, at deployed state, weight W, actuator's force F_a, slider displacement, Δl, and relative cable length variation, Δl_c

L_i [m]	Number of bars	System typology	V_S [m^3]	A_S [m^2]	W [kg]	F_a [kN]	Δl [m]	Δl_c [cm]
9.0	6	SS	0.20	11.16	49.50	2.40	2.64	
		CHS	0.64	8.26	110.31	0.98		34.70
	9	SS	0.20	11.35	49.50	3.10		
		HS	1.30	7.28	106.74	2.66	1.93	45.50
		CHS	0.66	8.66	123.31	1.53		10.50
	12	SS	0.20	11.42	49.50	2.12		
		HS	1.35	7.34	110.50	2.75	1.46	39.20
		CHS	0.67	8.81	138.00	0.92		7.50
12.0	8	SS	0.26	20.03	66.00	5.52		
		HS	1.71	14.32	136.48	3.81	2.87	68.40
		CHS	0.89	16.26	147.07	1.14		23.00
	12	SS	0.26	20.13	66.00	4.96		
		HS	1.80	14.52	141.63	3.90	1.96	40.90
		CHS	0.92	16.63	164.42	1.82		9.20
	16	SS	0.26	20.34	66.00	5.61		
		HS	1.84	14.75	146.50	4.08	1.49	49.10
		CHS	0.92	16.94	184.00	2.51		12.70
15.0	10	SS	0.33	31.43	82.50	8.82		
		HS	2.20	24.16	170.22	5.67	2.96	54.50
		CHS	1.14	26.84	183.84	2.50		15.90
	15	SS	0.33	31.78	82.50	8.61		
		HS	2.29	24.64	176.50	5.77	2.12	29.90
		CHS	1.16	27.48	205.52	4.73		6.50
	20	SS	0.33	31.80	82.50	8.11		
		HS	2.32	24.70	182.50	5.99	1.56	29.90
		CHS	1.17	27.63	230.00	5.30		4.20

the slider displacement and the relative cable length variation. It should be noted that the HS of 9.0 m initial length and the lowest number of bars, i.e., 6 bars, is unable to complete the deployment process, due to contact (i.e., geometrical incompatibility detected as part of motion planning) between the upper cable and the rigid bar of the linkage. Thus, this reconfiguration is not considered in the analysis. In the SS, the actuator's force corresponds to the horizontal component at the associated ground support, in the hybrid systems, the actuator's force is equal to the associated cable axial force. Thus, in the hybrid systems, the actuator's force, i.e., the transforming force, is superimposed over the cable pretension.

Among each system typology of same initial length, the structure volume of the SS remains

constant regardless of the number of bars used, whereas the structure volume of the hybrid systems at the deployed state increases depending on the number of bars used. Similarly, the enclosed area of the system typologies increases depending on the number of bars used. This value indicates the interior volume of the spatial building structure that would be defined by a flexible membrane envelope attached to the lower part of the structure. While all SS of equal initial length have the same self-weight regardless of the number of bars, the self-weight of the hybrid systems increases depending on the number of bars used, due to the respective increase of the required number of struts and the length of the cables. Among the SS of same initial length, the maximum actuator's force is lower with higher number of bars, except in the case of the SS of 12 m initial length and 12 bars, which has the lowest value. On the contrary, the hybrid systems require reduced maximum actuator's force with low number of bars. The highest maximum slider displacement is again lower with higher number of bars among all systems of same initial length. The same applies to the relative cable length variation of the hybrid systems, except in the case of the systems of 12 m initial length and 12 bars, which have registered the lowest respective values.

A comparison between the different system typologies of same initial length reveals that the SS has the lowest structure volume, and the HS, the highest. The maximum enclosed area is provided by the SS, followed by the CHS. Furthermore, the SS have the lowest self-weight, while the CHS the highest. The respective highest increase amounts to approximately 180 % in the case of the highest number of bars used in the systems, i.e., SS and CHS of 15 m initial length and 20 bars. Among the hybrid systems, the respective highest increase in self-weight amounts to 26 % in the same case. In all cases, the SS required the highest maximum actuator's force, while the CHS, the lowest. The CHS also recorded considerably lower maximum relative cable length variations compared to the HS.

The structural analysis results, with regard to the members bending moments, forces and system deformations, primarily highlight the significance of having minimum self-weight of the bar linkages. Further to the comparatively higher actuator's force required in the initial reconfiguration steps of the systems, the maximum deformations are also higher due to the systems almost flat shape, and the maximum bending moments and shear forces develop in the members close to the supports. Approaching the arch-like target shape, the maximum deformations reduce, and the maximum bending moments and shear forces develop in the middle members. The opposite applies to the members' axial forces, i.e., the flatter the positions of a system, the higher the axial forces develop in the central members, once the system has obtained the arch-like target shape, the maximum forces are transferred to the members close to the supports. At the target systems position, the respective inner forces of the secondary systems develop in the upper members, as opposed to where they appear at the beginning of deployment, namely, in the lower members.

Among the SS of 9.0 m initial length, the one with the highest number of bars, i.e., 12 bars, has the highest maximum bending moment of 0.51 kNm at the joint between the sixth and seventh beam and shear force of 0.24 kN in the beam connected to the sliding block. The same system also has the highest maximum deformation of 1.06 cm. The SS with 9 bars has the highest maximum axial force of 3.11 kN in the beam connected to the fixed support.

Among the HS of same initial length, the HS with lower feasible number of bars, i.e., 9 bars, has the highest maximum bending moment of 0.33 kNm in the beam connected to the sliding block, shear force of 0.68 kN in the fifth beam and axial force of 3.79 kN in the seventh beam. The same system also has the highest maximum bending moment of 0.08 kNm and shear force of 0.16 kN developed in the eighth lower strut. The HS with the highest number of bars has the highest

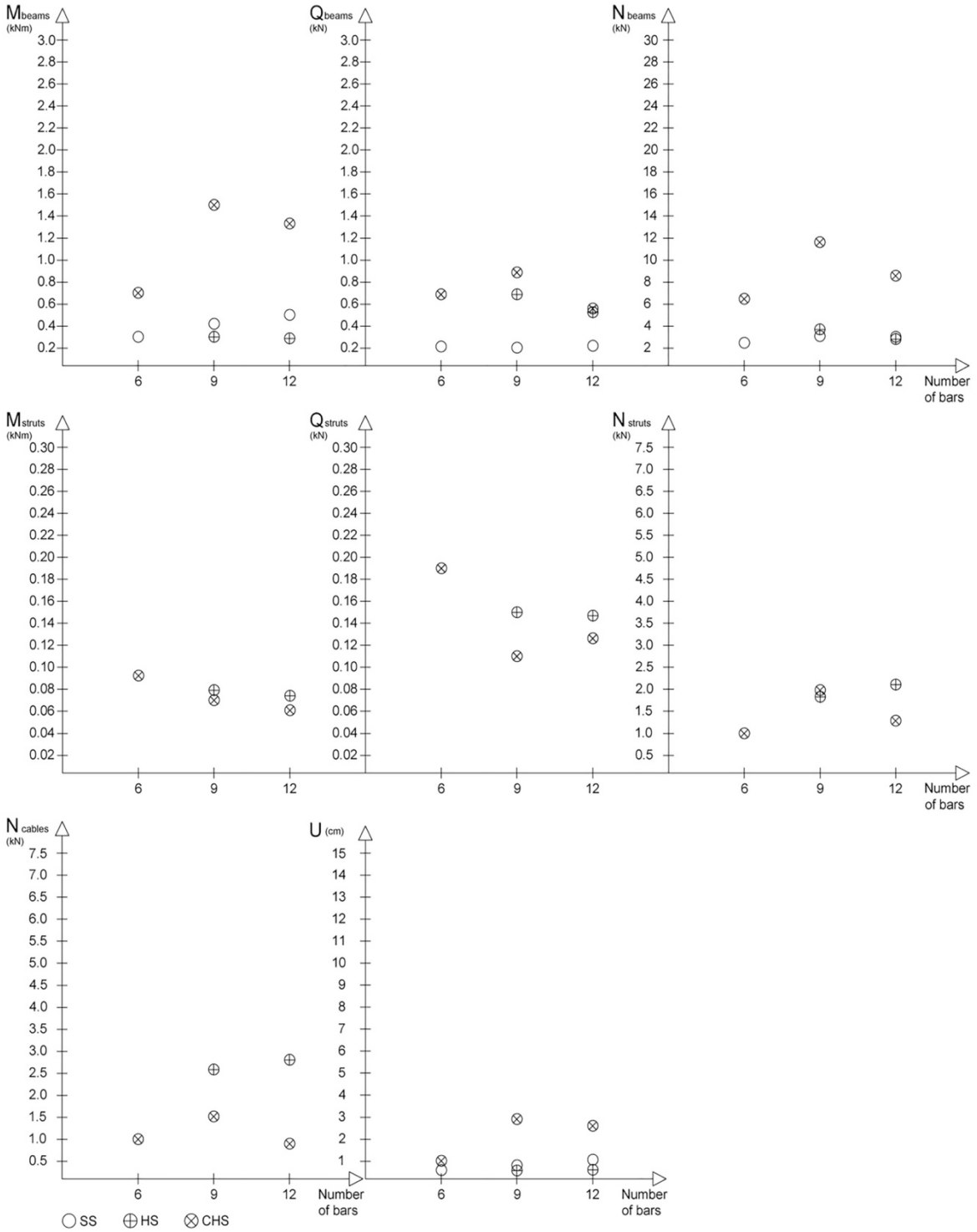

Fig. 8 Analysis results of bar linkages of initial system length of 9.0 m

maximum axial force of 2.13 kN in the first lower strut, as well as axial cable force of 2.75 kN in the lower cable. The same system has maximum deformation of 0.47 cm.

Among the CHS of same initial length, the one with 9 bars has the highest maximum bending moment of 1.55 kNm in the central beams, shear force of 0.86 kN in the second beam and axial force of 11.76 kN in the beam connected to the sliding block. The same system also has the highest maximum axial force of 1.97 kN developed in the second upper strut, axial cable force of 1.52 kN, in the lower cable, and deformation of 2.90 cm. The CHS with the lowest number of bars has the highest maximum bending moment of 0.09 kNm and shear force of 0.19 kN, both developed in the fourth upper strut.

A comparison between the systems of 9.0 m initial length reveals that the CHS with 9 bars has the highest maximum bending moment and inner forces in the beams, as well as deformation. The HS with 9 bars has the highest maximum bending moment and shear force in the struts. To the contrary, the HS with the highest number of bars has the highest maximum axial force in the struts and cables. The analysis results for the system typologies of this group are presented Fig. 8.

Among the SS of initial length of 12.0 m, the one with the highest number of bars, i.e.,16 bars, has the highest maximum bending moment of 0.95 kNm at the joint between the eighth and ninth beam, shear force of 0.32 kN in the beam connected to the sliding block and axial force of 5.62 kN in the beam connected to the fixed support. The same system also has the highest maximum system deformation of 3.40 cm.

Among the HS of same initial length, the one with the lowest number of bars, i.e., 8 bars, has the highest maximum bending moment of 0.59 kNm developed in the beam connected to the sliding block. The same system also has highest maximum bending moment of 0.15 kNm and shear force of 0.30 kN in the third lower strut. However, the system with the highest number of bars has the highest maximum shear force of 0.85 kN in the beam connected to the fixed support and axial force of 5.79 kN in the tenth beam. This system also has the highest maximum axial force of 3.19 kN in the first lower strut, axial cable force of 4.08 kN in the lower cable. The HS with the highest number of bars has maximum deformation of 1.10 cm.

Among the CHS of same initial length, the one with the highest number of bars has the highest maximum bending moment of 2.15 kNm at the joint between the eighth and ninth beam, shear force of 0.76 kN in the fourth beam and axial force of 15.31 kN in the beam connected to the sliding block. The same system has the highest maximum axial force of 3.73 kN in the lower strut, as well as the highest maximum axial cable force of 2.51 kN in the upper cable. The CHS with the lowest number of bars has the highest maximum bending moment of 0.09 kNm, shear force of 0.19 kN, both in the fifth upper strut. The CHS with the highest number of bars has maximum deformation of 7.50 cm.

A comparison between the systems of 12.0 m initial length reveals that the CHS with the highest number of bars has the highest maximum bending moment and axial force in the beams, as well as axial force in the struts. The same system has maximum deformation. The highest maximum shear force in the beams and axial cable force are developed in the HS with the highest number of bars. The highest maximum bending moment and shear force in the struts are developed in the HS with the lowest number of bars. The analysis results for the system typologies of this group are presented in Fig. 9.

Among the SS of 15.0 m initial length, the one with the highest number of bars, i.e., 20 bars, has the highest maximum bending moment of 1.49 kN in the tenth beam and shear force of 0.40 kN in the beam connected to the sliding block. The same system also has the highest maximum deformation of 8.39 cm. The SS with the lowest number of bars, i.e., 10 bars, has the highest

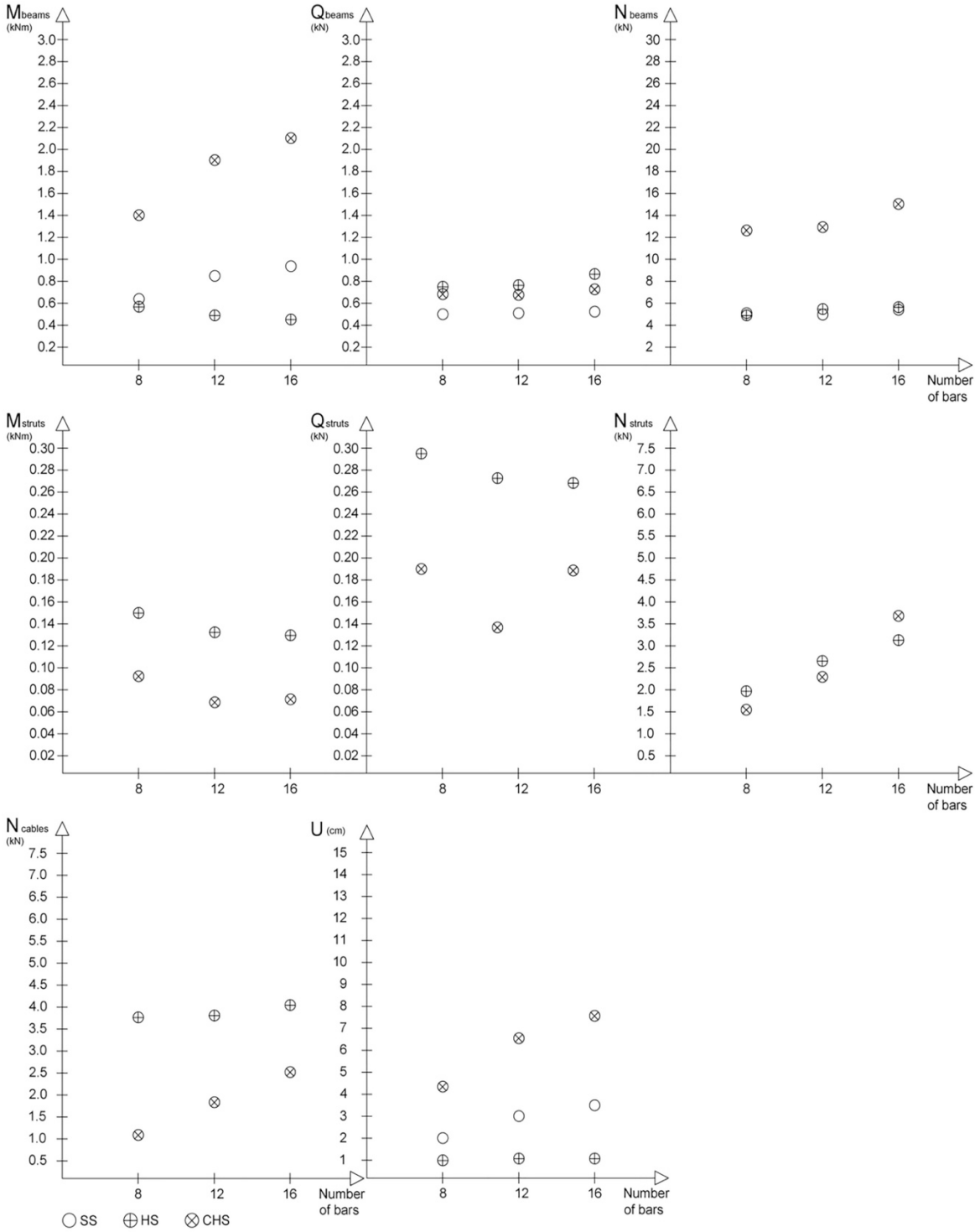

Fig. 9 Analysis results of bar linkages of initial system length of 12.0 m

maximum axial force of 8.83 kN in the beam connected to the fixed support.

Among the HS of same initial length, the one with the lowest number of bars, i.e., 10 bars, has the highest maximum bending moment of 0.87 kNm in the beam connected to the fixed support. The system with the highest number of bars has the highest maximum shear force of 1.20 kN in the beam connected to the fixed support and axial force of 8.78 kN in the eleventh beam. The same system has the maximum axial force of 4.50 kN in the first lower strut and axial cable force of 5.99 kN in the lower cable. The HS with 15 bars has the highest maximum bending moment of 0.23 kNm and shear force of 0.47 kN in the third lower strut. The same system has maximum deformation of 2.20 cm.

Among the CHS of same initial length, the one with the highest number of bars has the highest maximum response values of the beams, the highest maximum bending moment of 2.43 kNm is developed in the eleventh beam, shear force of 0.92 kN in the fourth beam, and axial force of 22.52 kN in the beam connected to the sliding block. With regard to the secondary system, the highest maximum bending moment of 0.12 kNm and shear force of 0.25 kN are developed in the sixteenth lower strut, as well as the axial force of 9.93 kN, in the first lower strut. The particular system has the highest maximum axial cable force of 5.30 kN in the lower cable, as well as deformation of 13.70 cm.

A comparison between the systems of 15.0 m initial length reveals that the CHS with the highest number of bars has the highest maximum bending moment and axial force in the beams, as well as axial force in the struts. The same system has maximum deformation. The HS with the highest number of bars has the highest maximum shear force in the beams, as well as axial cable force. The HS with the lowest number of bars has the highest maximum bending moment and shear force in the struts. The analysis results for the system typologies of this group are presented in Fig. 10.

A comparative analysis of the system typologies with regard to a respective increase of the number of bars of equal length exemplifies the related systems behavior. The linkages with individual bar length of 1.5 m refer to the 6, 8 and 10-bar systems, the ones with individual bar length of 1.0 m, to the 9, 12 and 15-bar systems, and those with individual bar length of 0.75 m, to the 12, 16 and 20-bar systems of 9.0, 12.0 and 15.0 m initial length, respectively. The systems highest maximum bending moments, cable axial forces and relative length variations, are shown in Fig. 11.

In all cases, the highest maximum bending moments in the beams involve the CHS. In the systems with individual bar length of 1.5 m, this typology also has the highest respective increase of 1.45 kNm as the number of units increases from 6 to 10. When the individual bar length decreases the respective increase rate in the CHS also decreases. Accordingly, in the other two individual bar length cases, the highest increase rates are registered by the SS. In all cases, the lowest respective values are registered in HS, according to the number of units.

With regard to the hybrid systems, in all cases, the highest cable axial forces are registered in the HS. Again, this typology with individual bar length of 1.5 m has the highest respective increase of 1.84 kN, with an increase in the number of units from 8 to 10. Along with the decrease of the individual bar length, the respective increase rate in the HS also decreases. Accordingly, in the other two individual bar length cases, the highest increase rates are recorded in the CHS.

The highest relative cable length variations are also recorded in the HS. In the systems with individual bar length of 1.5 and 1.0 m, the highest respective values decrease with the increase in the number of units, i.e., the respective values amount to 13.90 and 11.00 cm from 8 to 10 units and from 12 to 15 units respectively. However, in the hybrid systems with individual bar length of

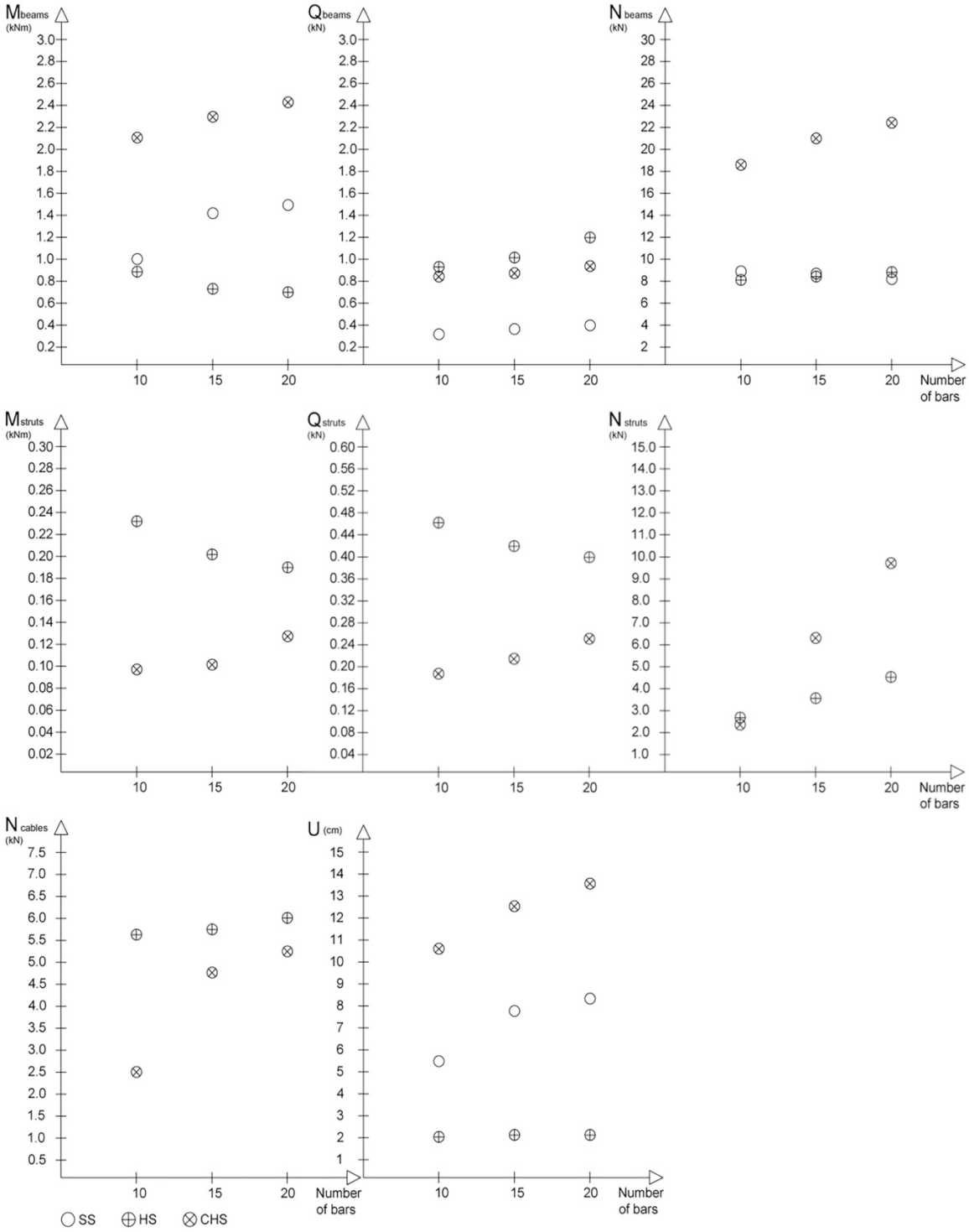

Fig. 10 Analysis results of bar linkages of initial system length of 15.0 m

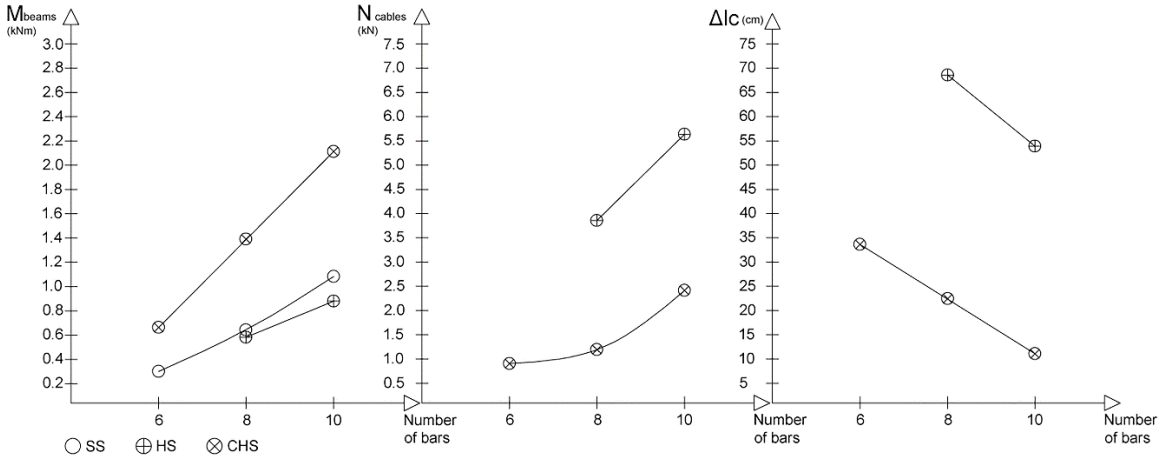

(a) Individual bar length of 1.5 m

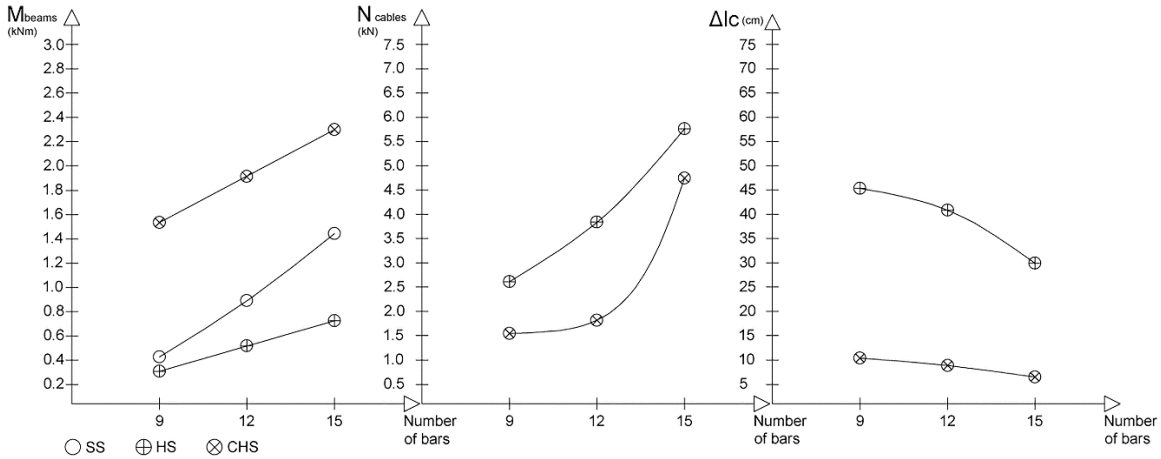

(b) Individual bar length of 1.0 m

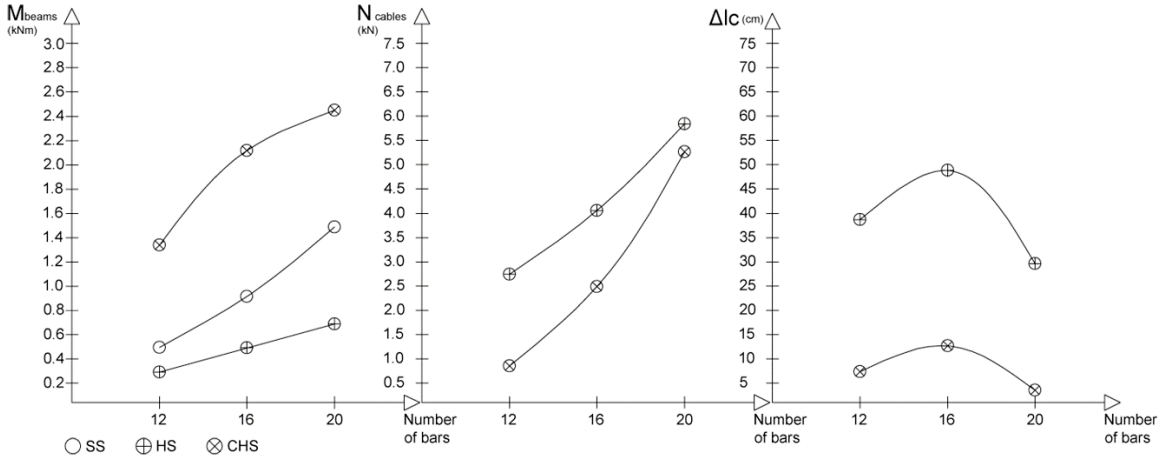

(c) Individual bar length of 0.75 m

Fig. 11 Analysis results of system typologies development

0.75 m, the highest maximum value is recorded in the systems with 16 bars. The lowest values are developed with higher number of bars.

Among the systems investigated, the SS have the advantage of lowest structure volume and minimum self-weight, as well as an increased interior volume of the building structure. Nevertheless, they require the highest maximum actuator's forces for the reconfiguration. On the contrary, the CHS have maximum self-weight, and combined with the lowest number of bars, they recorded the lowest maximum actuator's force and relative cable length variation for the reconfiguration. Likewise, the sliding block displacements decrease with the increase in the number of bars used in the systems. Furthermore, the highest maximum bending moment and axial force in the beams, as well as axial force in the struts, are developed in the CHS with the highest number of bars. The same system also has the highest maximum deformation. The highest maximum shear force in the beams, and axial cable force, are developed in the HS with the highest number of bars. The HS with 10 bars has the highest maximum bending moment and shear force in the struts. From a structural point of view, the CHS has higher bending moments in the beams induced by the pretension of the cables and their diagonal configuration, as well as the increase of the self-weight of the system. The HS succeeds in having low bending moments in the beams, which however occurs at the cost of high cable axial forces, i.e., actuator's forces, and relative cable length variations.

4. Conclusions

The current paper presents a deployment and reconfiguration approach for bar linkage structures based on the ECS method. The simulation study conducted refers to the preliminary kinematics analysis and the FEA of three groups of planar linkage systems, each with specific initial overall length and corresponding target span, different number of rigid bars and typologies, i.e., simple, hybrid and cross hybrid systems. The numerical results demonstrate the feasibility and potential of the proposed ECS approach and the efficiency of the hybridization concept for actuation purposes. Based on the specific case study, for a given initial length, the simple system requires lower maximum actuator's force with higher number of bars, while the hybrid systems require comparatively reduced actuator's force, especially with lower number of bars. Furthermore, the lowest sliding block displacements, and relative cable length variations, are required in the systems with higher number of bars. On the contrary, the highest maximum bending moment and inner forces in the members and system deformations are developed in the linkages with higher initial length and number of bars. Furthermore, only the hybrid system with horizontal cables effectively reduces the maximum bending moments of the primary members through the development of axial cable forces. However, the specific typology records increased actuator's forces and relative cable length variations compared to the one with diagonal cables, especially in the case with the lowest number of bars. It should also be noted that under realistic external loading conditions, the hybrid systems, and especially the CHS, are expected to have improved structural stiffness characteristics in the deployed state compared to the simple system. The main findings of this study need to be further examined through prototyping and experimental testing. Within this framework, effective designs may promote desirable features including modularity, ease of assembly, self-erectability, reconfigurability and structural reliability under varying loading conditions.

Acknowledgement

The research described in this paper was partially supported by the University of Cyprus (Roys Poyiadjis Academic Excellence Graduate Students Scholarship 2018-19).

References

Acharyya, S.K. and Mandal, M. (2009), "Performance of EAs for four-bar linkage synthesis", *Mech. Mach. Theory*, **44**, 1784-1794. https://doi.org/10.1016/j.mechmachtheory.2009.03.003.

Adam, B. and Smith, I.F.C. (2008), "Active tensegrity: A control framework for an adaptive civil-engineering structure", *Comp. Struct.*, **86**(23-24), 2215-2223. https://doi.org/10.1016/j.compstruc.2008.05.006.

Akgün, Y., Gantes, C.J., Kalochairetis, K. and Kiper, G. (2010), "A novel concept of convertible roofs with high transformability consisting of planar scissor-hinge structures", *Eng. Struct.*, **32**, 2873-2883. https://doi.org/10.1016/j.engstruct.2010.05.006.

Akgün, Y., Gantes, C.J., Sobek, W., Korkmaz, K. and Kalochairetis, K. (2011), "A novel adaptive spatial scissor-hinge structural mechanism for convertible roofs", *Eng. Struct.*, **33**(4), 1365-1376. https://doi.org/10.1016/j.engstruct.2011.01.014.

Alegria Mira, L., Filomeno Coelho, R., Thrall, A.P. and De Temmerman, N. (2015), "Parametric evaluation of deployable scissor arches", *Eng. Struct.*, **99**, 479-491. https://doi.org/10.1016/j.engstruct.2015.05.013

Bel Hadj Ali N., Rhode-Barbarigos L. and Smith I.F.C. (2011), "Analysis of clustered tensegrity structures using a modified dynamic relaxation algorithm", *Int. J. Solids Struct.*, **48**(5), 637-647. https://doi.org/10.1016/j.ijsolstr.2010.10.029.

Chen, Y., Fan, L., Bai, Y., Feng, J. and Sareh, P. (2020), "Assigning mountain-valley fold lines of flat-foldable origami patterns based on graph theory and mixed-integer linear programming", *Comput. Struct.*, **239**, 106328. https://doi.org/10.1016/j.compstruc.2020.106328.

Chen, Y., Fan, L. and Feng, J. (2017), "Kinematic of symmetric deployable scissor-hinge structures with integral mechanism mode", *Comput. Struct.*, **191**, 140-152. https://doi.org/10.1016/j.compstruc.2017.06.006.

Chen, Y., Feng, J. and Sun, Q. (2018), "Lower-order symmetric mechanism modes and bifurcation behavior of deployable bar structures with cyclic symmetry", *Int. J. Solids Struct.*, **139-140**, 1-14. https://doi.org/10.1016/j.ijsolstr.2017.05.008.

Chen, Y., Peng, R. and You, Z. (2015), "Origami of thick panels", *Science*, **349**(6246), 396-400. https://doi.org/10.1126/science.aab2870.

Chen, Y., Yan, J., Feng, J. and Sareh, P. (2021), "PSO-based metaheuristic design generation of non-trivial flat-foldable origami tessellations with degree-4 vertices", *J. Mech. Des.*, **143**(1), 011703. https://doi.org/10.1115/1.4047437.

Chen, Y. and You, Z. (2008), "On mobile assemblies of Bennett linkages", *Proceedings of the Royal Society of Automotive Engineers*, **464**(2093), 1275-1293. https://doi.org/10.1098/rspa.2007.0188.

Christoforou, E.G., Müller, A., Phocas, M.C., Matheou, M. and Arnos, S. (2015), "Design and control concept for reconfigurable architecture", *J. Mech. Des.*, **137**, 042302. https://doi.org/10.1115/1.4029617.

Christoforou, E.G., Phocas, M.C., Matheou, M. and Müller, A. (2019), "Experimental implementation of the 'effective 4-bar method' on a reconfigurable articulated structure", *Struct.*, **20**, 157-165. https://doi.org/10.1016/j.istruc.2019.03.009.

Djouadi, A., Motro, R., Pons, J.C. and Crosnier, B. (1998), "Active control of tensegrity systems", *Aerospace Eng.*, **11**, 37-44. https://doi.org/10.1061/(ASCE)0893-1321(1998)11:2(37).

Doroftei, I., Oprisan, C. and Popescu, A. (2014), "Deployable structures for architectural applications – A short review", *Appl. Mech. Mat.*, **658**, 233-240. https://doi.org/10.4028/www.scientific.net/AMM.658.233.

Engel, H. (2009), *Structure Systems*, Hatje Cantz, Stuttgart, Germany.

Escrig, F. (1985), "Expandable space structures", *Int. J. Space Struct.*, **2**(1), 79-91. https://doi.org/10.1177%2F026635118500100203.

Fontes, J.V. and da Silva, M.M. (2016), "On the dynamic performance of parallel kinematic manipulators with actuation and kinematic redundancies", *Mech. Mach. Theory*, **103**, 148-166. https://doi.org/10.1016/j.mechmachtheory.2016.05.004.

Gan, W.W. and Pellegrino, S. (2003), "Closed-loop deployable structures", *Proceedings of the 44th AIAA/ASME/ASCE/AHS/ASC Structures, Structural Dynamics and Materials Conference,* Norfolk, Virginia, U.S.A., April. https://doi.org/10.2514/6.2003-1450.

Gantes, C.J. (2001), *Deployable Structures: Analysis and Design*, WIT Press, Southampton, U.K.

Georgiou, N. and Phocas, M.C. (2020), "Kinematics analysis of deployable and reconfigurable bar-linkage structures", *Proceedings of the 2020 Structures Congress, Structures 20, 2020 International Conference on Advances in Computational Design*, Seoul, Korea, August.

Gogu, G. (2005), "Mobility of mechanisms: a critical review", *Mech. Mach. Theory*, **40**, 1068-1097. https://doi.org/10.1016/j.mechmachtheory.2004.12.014.

Hanaor, A. (1998), *Tensegrity. Theory and application*, Beyond the Cube, John Wiley & Sons, New York, U.S.A.

Hanaor, A. and Levy, R. (2001), "Evaluation of deployable structures for space enclosures", *Int. J. Space Struct.*, **16**(4), 211-229. https://doi.org/10.1260%2F026635101760832172.

Hoberman, C. (1993), "Unfolding architecture: An object that is identically a structure and a mechanism", *Arch. Des.*, **63**, 53-59.

Jensen, F.V. (2005), "Concepts for retractable roof structures", Ph.D. Dissertation, University of Cambridge, Cambridge, U.K. https://doi.org/10.17863/CAM.14143.

Krishnan, S. and Liao, Y. (2020), "Geometric design of deployable spatial structures made of three-dimensional angulated members", *J. Archit. Eng.*, **26**(3), 04020029. https://doi.org/10.1061/(ASCE)AE.1943-5568.0000416.

Li, S., Fang, H., Sadeghi, S., Bhovad, P. and Wang, K.W. (2019), "Architected origami materials: How folding creates sophisticated mechanical properties" *Adv. Mater.*, **31**(5), 1805282. https://doi.org/10.1002/adma.201805282.

Lin, F., Chen, C., Chen, J. and Chen, M. (2019), "Modelling and analysis for a cylindrical net-shell deployable mechanism", *Adv. Struct. Eng.*, **22**(15), 3149-3160. https://doi.org/10.1177%2F1369433219859400.

Maden, F., Korkmaz, K. and Akgün, Y. (2011), "A review of planar scissor structural mechanisms: Geometric principles and design methods", *Arch. Sci. Rev.*, **54**, 246-257. https://doi.org/10.1080/00038628.2011.590054.

Matheou, M., Phocas, M.C., Christoforou, E.G. and Müller, A. (2018), "On the kinetics of reconfigurable hybrid structures", *J. Build. Eng.*, **17**, 32-42. https://doi.org/10.1016/j.jobe.2018.01.013.

Melancon, D., Gorissen, B., García-Mora, C.J., Hoberman, C. and Bertoldi, K. (2021), "Multistable inflatable origami structures at the metre scale", *Nature*, **592**, 545-550. https://doi.org/10.1038/s41586-021-03407-4.

Moored, K.W. and Bart-Smith, H. (2009), "Investigation of clustered actuation in tensegrity structures", *Int. J. Solids Struct.*,**46**(18), 3272-3281. https://doi.org/10.1016/j.ijsolstr.2009.04.026.

Moored, K.W., Kemp, T.H., Hole, N.E. and Bart-Smith, H. (2011), "Analytical predictions, optimization and design of a tensegrity-based artificial pectoral fin", *Int. J. Solids Struct.*, **48**(22-23), 3142-3159. https://doi.org/10.1016/j.ijsolstr.2011.07.008.

Motro, R., Bouderbala, M., Lesaux, C. and Cevaer, F. (2001), *Foldable Tensegrities, Deployable Structures*, Springer, Vienna, Austria. https://doi.org/10.1007/978-3-7091-2584-7_11.

Müller, A. (2005), "Internal preload control of redundantly actuated parallel manipulators - Its application to backlash avoiding control", *IEEE T. Robot.*, **21**(4), 668-677. https://doi.org/10.1109/TRO.2004.842341.

Müller, A. (2013), "On the terminology and geometric aspects of redundantly actuated parallel manipulators", *Robotica*, **31**(1), 137-147. https://doi.org/10.1017/S0263574712000173.

Norton, R. (2008), *Design of Machinery*, McGraw-Hill, New York, U.S.A.

Park, F.C. and Kim, J.W. (1999), "Singularity analysis of closed kinematic chains", *J. Mech. Des.*, **121**(1), 32-38. https://doi.org/10.1115/1.2829426.
Pellegrino, S. (2001), "Deployable structures", *CIMS Int. Center Mech. Sci.,* **412**. http://doi.org/10.1007/978-3-7091-2584-7.
Pérez-Valcárcel, J., Munõz-Vidal, M., Suárez-Riestra, F., López-César, I.R. and Freire-Tellado, M.J. (2021), "A new system of deployable structures with reciprocal linkages for emergency buildings", *J. Build. Eng.*, **33**, 101609. https://doi.org/10.1016/j.jobe.2020.101609.
Phocas, M.C., Alexandrou, K. and Athini, S. (2019), "Design and analysis of an adaptive hybridstructure of linearly interconnected scissor-like and cable bending-active components", *Eng. Struct.*, **192**, 156-165. https://doi.org/10.1016/j.engstruct.2019.04.102.
Phocas, M.C., Christoforou, E.G. and Dimitriou, P. (2020), "Kinematics and control approach for deployable and reconfigurable rigid bar linkage structures", *Eng. Struct.*, **208**, 110310. https://doi.org/10.1016/j.engstruct.2020.110310.
Phocas, M.C., Christoforou, E.G. and Matheou, M. (2015), "Design, motion planning and control of a reconfigurable hybrid structure", *Eng. Struct.*, **101**(10), 376-385. https://doi.org/10.1016/j.engstruct.2015.07.036.
Phocas, M.C., Kontovourkis, O. and Matheou, M. (2012), "Kinetic hybrid structure development and simulation", *Int. J. Arch. Comp.*, **10**(1), 67-86. https://doi.org/10.1260%2F1478-0771.10.1.67.
Phocas, M.C., Matheou, M., Müller, A. and Christoforou, E.G. (2019), "Reconfigurable modular bar structure", *J. Int. Assoc. Shell Spatial Struct.*, **60**(1), 78-89. https://doi.org/10.20898/j.iass.2019.199.028.
Phukaokaew, W., Sleesongsom, S., Panagant, N. and Bureerat, S. (2019), "Synthesis of four-bar linkage motion generation using optimization algorithms", *Adv. Comput. Des.*, **4**(3), 197-210. https://doi.org/10.12989/acd.2019.4.3.197.
Pugh, A. (1976), *An Introduction to Tensegrity*, University of California Press, Berkeley, U.S.A.
Rhode-Barbarigos, L. (2012), "An active deployable structure", Ph.D. Dissertation, EPFL, Lausanne, Switzerland.
Richard Liew, J.Y., Vu, K.K. and Krishnapillai, A. (2008), "Recent development of deployable tension-strut structures", *Adv. Struct. Eng.*, **11**(6), 599-614. https://doi.org/10.1260%2F136943308787543630.
Rivas-Adrover, E. (2018), "A new hybrid type of deployable structure: Origami-scissor hinged", *J. Int. Assoc. Shell Spatial Struct.*, **59**(3), 183-190. https://doi.org/10.20898/j.iass.2018.197.010.
Roovers, K. and De Temmerman, N. (2017), "Deployable scissor grids consisting of translational units", *Int. J. Solids Struct.*, **121**, 45-61. https://doi.org/10.1016/j.ijsolstr.2017.05.015.
Saitoh, M. and Okada, A. (1999), "The role of string in hybrid string structure", *Eng. Struct.*, **21**, 756-769. https://doi.org/10.1016/S0141-0296(98)00029-7.
Schenk, M., Guest, S.D. and Herder, J.L. (2007), "Zero stiffness tensegrity structures", *Int. J. Solids Struct.*, **44**(20), 6569-6583. https://doi.org/10.1016/j.ijsolstr.2007.02.041.
Schlaich, J., Bergermann, R., Boegle, R., Cachola, A. and Flagge, S.P. (2005), *Light Structures*, Prestel, New York, U.S.A.
Snelson, K. (1965), *Continuous Tension, Discontinuous Compression Structures*, U.S. Patent No. 3,169,611, Washington, D.C., U.S.A.
Thrall, A.P., Adriaenssens, S., Paya-Zaforteza, I. and Zoli, T.P. (2012), "Linkage-based movable bridges: Design methodology and three novel forms", *Eng. Struct.*, **37**, 214-223. https://doi.org/10.1016/j.engstruct.2011.12.031.
Tibert, G. (2002), "Deployable tensegrity structures for space applications", Ph.D. Dissertation, Stockholm Royal Institute of Technology, Stockholm, Switzerland.
You, Z. and Pellegrino, S. (1997), "Foldable bar structures", *Int. J. Solids Struct.*, **15**(34), 1825-1847. https://doi.org/10.1016/S0020-7683(96)00125-4.